Large scale indium tin oxide (ITO) one dimensional gratings for ultrafast signal modulation in the visible

Michele Guizzardi[1], Silvio Bonfadini[1,2], Liliana Moscardi[1,2], Ilka Kriegel[3], Francesco Scotognella[1,2], Luigino Criante[2]
[1]*Dipartimento di Fisica, Politecnico di Milano, Piazza Leonardo da Vinci 32, 20133 Milano, Italy*
[2]*Center for Nano Science and Technology@PoliMi, Istituto Italiano di Tecnologia, Via Giovanni Pascoli, 70/3, 20133, Milan, Italy*
[3]*Department of Nanochemistry, Istituto Italiano di Tecnologia (IIT), via Morego, 30, 16163 Genova, Italy*
*email address: francesco.scotognella@polimi.it

Abstract
Indium Tin Oxide (ITO) is a heavily doped semiconductor with a plasmonic response in the near infrared. When exposed to light, the distribution of conduction band electron induces a change in the real and imaginary parts of the dielectric permittivity. The coupling of the electromagnetic waves with the electrons in the conduction band of metallic nanostructures with ultrashort light pulses results in nonlinear plasmonic response Such optical modulation occurring on ultrafast time scales, e.g. picosecond response times can be exploited and used to create integrated optical components with terahertz modulation speed. Here, we present a photophysical study on an ITO one dimensional grating, realized using femtosecond micromachining technology, a technology very industrially accessible. The geometries, dimensions and pitch of the various gratings analyzed are obtained by means of direct ablation in a controlled atmosphere of a homogeneous thin layer of ITO deposited on a glass substrate. The pitch has been selected in order to obtain a higher order of the photonic band gap in the visible. Femtosecond micromachining technology guarantees precision, repeatability and extreme manufacturing flexibility. By means of ultrafast pump-probe spectroscopy we characterize both the plasmon and inter-band temporal dynamics. We observe a large optical non-linearity of ITO grating in the visible range, where the photonic band gap occurs, when pumped at the surface plasmon resonance in the near infrared (1500 nm). All together we show the possibility of all-optical signal modulation with heavily doped semiconductors in their transparency window with a picosecond response time through the formation of ITO grating structures.

Introduction
Heavily doped semiconductors are materials in which the carrier density is few orders of magnitude below the ones of metals [1–6]. Thus, these materials show a metallic behavior with a good conductivity. The plasmonic resonance is shifted to lower energies, mostly in the near infrared spectral range, and therefore heavily doped semiconductors display transparency in the visible, hence the term transparent conducting oxides. Transparent conductive oxides are a famous class of heavily doped semiconductors that find wide application for optical and optoelectronic device fabrication [7,8]. Indium tin oxide (ITO) is one of most used transparent conductive oxide and has a carrier density ranging from about $1.5 \times 10^{20}\ carriers/cm^{-3}$ to about $3.5 \times 10^{21}\ carriers/cm^{-3}$ [1].
The ultrafast optical nonlinearity in ITO has been studied highlighting its epsilon-near-zero region [9]. Very interesting samples are the arrays of ITO nanostructures. In 2014, a plasmonic-photonic mode coupling has been observed in ITO nanorod arrays [10]. Ultrafast switching in ITO nanorod arrays has been observed in 2014 [11] and in 2016 [12]. Moreover, with a precise fabrication of the

ITO nanorod arrays, sub-picosecond all-optical modulation has been demonstrated in the visible spectral region [13,14]. The ITO nanorod arrays have been fabricated by electron beam lithography and it is interesting to pursue other ways to fabricated periodic arrangements of ITO at a length scale comparable with visible and near infrared wavelengths. Just as an example, ultrafast modulation has been demonstrated also in ITO/SiO_2 multilayer photonic crystals [15].
We present here the fabrication of ITO gratings by means of femtosecond laser micromachining a technology which is very relevant for industrial application. The transient response of ITO and relative gratings was studied by ultrafast pump-probe transient absorption measurements. To fully characterize intra and interband carrier dynamics we performed two different experiments. When the sample is excited via an intraband excitation we see an ultrafast modulation of the photonic band gap of the ITO grating that is induced by the Fermi gas heating with picosecond response time. On the other hand, the interband excitation results in the formation of long living states that we ascribe to electron traps at the material surface, possibly generated in the fabrication process.

Methods

Fabrication: the patterning of ITO substrate was performed using a femtosecond (fs) laser micromachining. This maskless technique is based on non-linear processes, such as multiphoton absorption, which allows a high controlled energy deposition in automatic way also. The system is based on a mode-locked solid-state laser source (Yb:KGW active medium, Pharos by Light Conversion) with a regenerative amplifier. Emitted pulses are characterized by wavelength of 1030 nm, duration of 240 fs, repetition rate up to 1 MHz and pulse energy up to 0.2 mJ. The laser radiation can be modified in wavelength, thanks to the external harmonic generator (2^{nd}, 3^{rd} and 4^{th}, HIRO by Light Conversion), intensity and polarization. The pulsed light is then statically focused on the substrate surface (1.1 mm thickness) with a 20X - 0.4 NA microscope objective (M Plan Apo SL20X Ultra-Long Working Distance Plan-Apochromat, Mitutoyo). Computer-controlled, high precision 3-axis motion stages (air-baring ABL-1000, Aerotech) interfaced by CAD-based software (ScaBase, Altechna) with an integrated acousto-optic modulator are used to translate the sample relative to the laser irradiation desiderate pattern of the sample. It is well known that direct laser ablation typically creates a large number of debris. In order to overcome those problems a particular precaution has been used: the sample has placed in a controlled atmosphere chamber in which the working condition is maintained slightly below the atmosphere pressure (2×10^{-2} bar) via a flux provided by a gas tank and a vacuum pump [16]. The low pressure avoids the debris deposition and significantly improve the ablation quality by promoting the separation of the ablated material from the crystal bulk. In this way the low size debris created by femtosecond ablation (tens of nanometers in diameter) are free to "fly" away from the unprocessed area thanks to the increase in their average free path and to the low kinetic energy possessed.
Samples characterization: the scanning electron microscope characterization of 1D pattern has been conducted with a Joel SEM. The measurement has been performed at a voltage of 5 kV and backscattered electrons have been detected. The optical transmission spectrum of the photonic crystal has been measured with a Perkin Elmer spectrophotometer Lambda 1050 WB over the full working range, from 200 nm up to 3300 nm.
Pump probe experiments: For intraband pumping of ITO we use a non-collinear optical parametric amplifier (OPA) tuned at 1500 nm, which permits resonance absorption in the metallic region of the ITO (plasmon resonance). To excite the interband transition of ITO, taking into account that the electronic bandgap of ITO is around 3.6 eV, we utilize the third harmonic of the fundamental (800nm) and we generate 266nm (4,65 eV). The pump pulses are focused to a 400 µm diameter spot. A white light probe is generated by focusing the laser into a sapphire plate, covering the range

of 400-700nm and focused on the sample. A chirp-free differential transmission, $\frac{\Delta T(t)}{T} = \frac{T_{ON}(t) - T_{OFF}}{T_{OFF}}$, spectra are collected by using an optical multichannel analyzer with a dechirping algorithm [17].

Results and discussion

Sample fabrication and characterization

The gratings have been fabricated by femtosecond laser micromachining via ablation of a commercial ITO thin film deposited on a glass substrate (ITO-15 Glass 1.1mm, XOP FÍSICA SL). A square area of 5x5 mm was patterned with a 1D periodic structure composed by lines separated by an empty space, as shown in Figure 1a. To fabricate this pattern we use the fundamental of the laser (1030 nm) at a repetition rate of 500 kHz, while to obtain a clear ablation line around 4 µm wide, we use an average power of 120 mW and 20000 pulses/mm. We have realized two periodic patterns, with periods Λ=6 µm (Figure 1c and d) and Λ=9 µm (Figure 1e and f). The distance between ablation lines has been engineered to be around 1.5 µm and 1.9 µm as dimension of the periodic ITO line (*d*) of the 6 µm and 9 µm pattern periods, respectively. It is noteworthy to underline that with this technique it is possible to achieve a very high homogeneity of the sample over a large area with at least millimeter dimensions.

After the ablation the sample has been cleaned in ultrasonic bath of water and isopropanol mixed solution to remove possible remaining debris. The obtained ITO pattern has been quality controlled in its dimensions using a Scanning Electron Microscope (SEM). Different scale SEM images of patterns are reported in Figure 1 (c-f). The optical properties of the ITO, patterned or not patterned films, have been initially investigated by measuring the transmission spectra in the range of 220 nm up to 1000 nm. Machined ITO shows a clear change in the spectral transmission in the visible spectral range compared to the pure substrate, as reported in Figure 1b. This variation in optical signal is ascribed to the appearance of the photonic stop band of the grating due to the periodic arrangement of the structure.

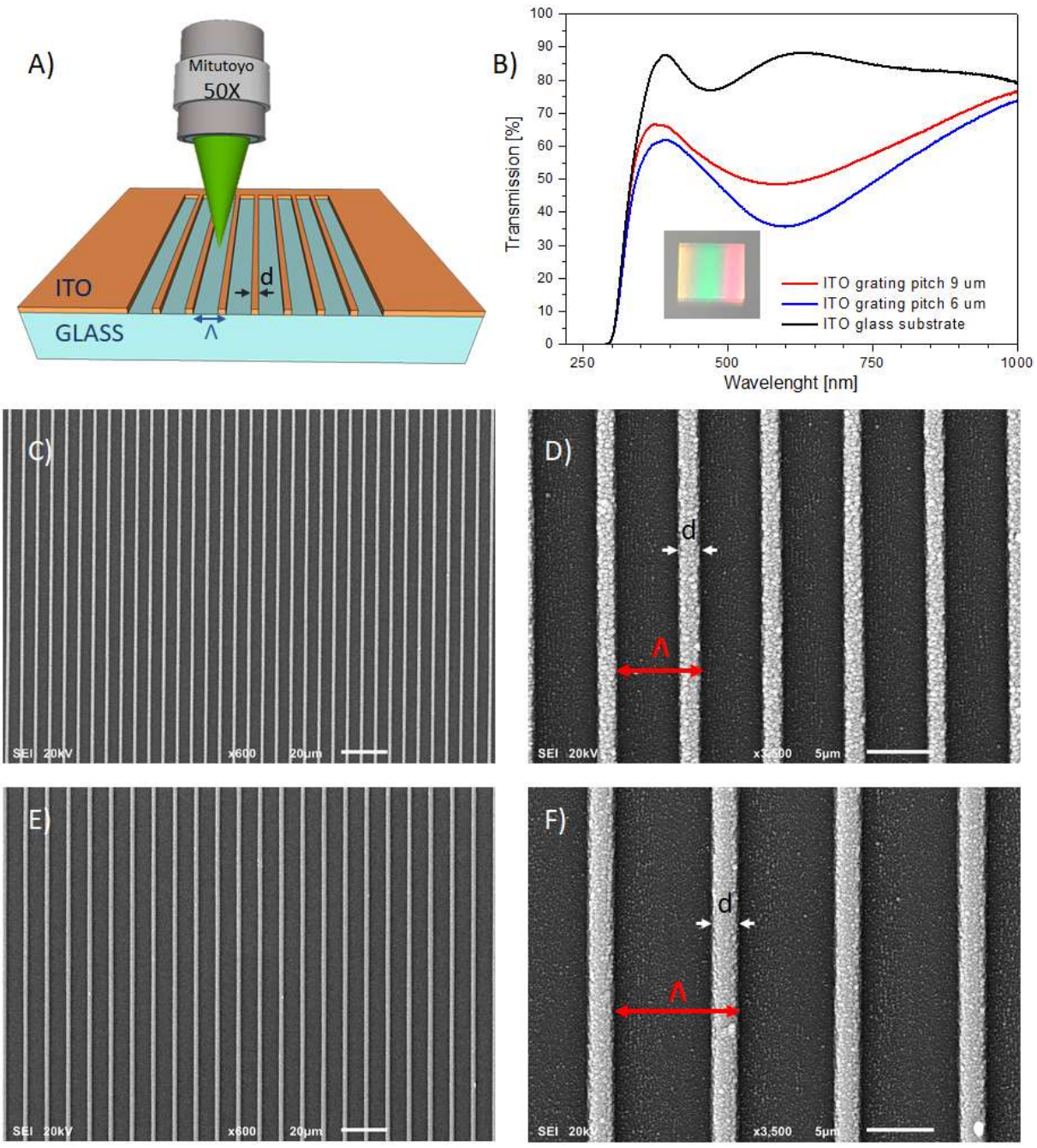

Figure 1 Sketch of the ITO pattern made by femtosecond-laser fabrication (a). Transmission spectra comparation of pure ITO glass substrate, patterned ITO areas (capture) with pitch of 6 µm and 9 µm (b). Different scale SEM images of the two patterns fabricated, w with pitch Λ=6 µm and d=1.5 µm (c and d) and Λ=9 µm and d=1.9 µm (e and f).

For comparison we also measured the transmission spectra in the near infrared up to about 2200 nm (see Figure S2 of the Supporting Information), which shows that the ITO film is nearly transparent in the visible range, while in the infrared part of the spectra the presence of the plasmonic resonance decreases the transmission from 80% to below 10%. The valley at about 400 nm is due to the interband absorption of ITO. These results show clearly that the strong transmission dip around 600 nm is due to the microfabrication of the ITO patterns.

Ultrafast pump probe spectroscopy

To study the variation of the signal in our ITO gratings we chose two different excitation schemes: pumping at 1500 nm in order to achieve intraband excitation and 266 nm to excite the interband

transitions. First, we focus on the intraband excitation with an ultrashort pulse that is resonant with the plasmon resonance of the ITO and we study the reference ITO thin film without the grating structure. In Figure 2 we show the results of our intraband ultrafast experiment performed on ITO.

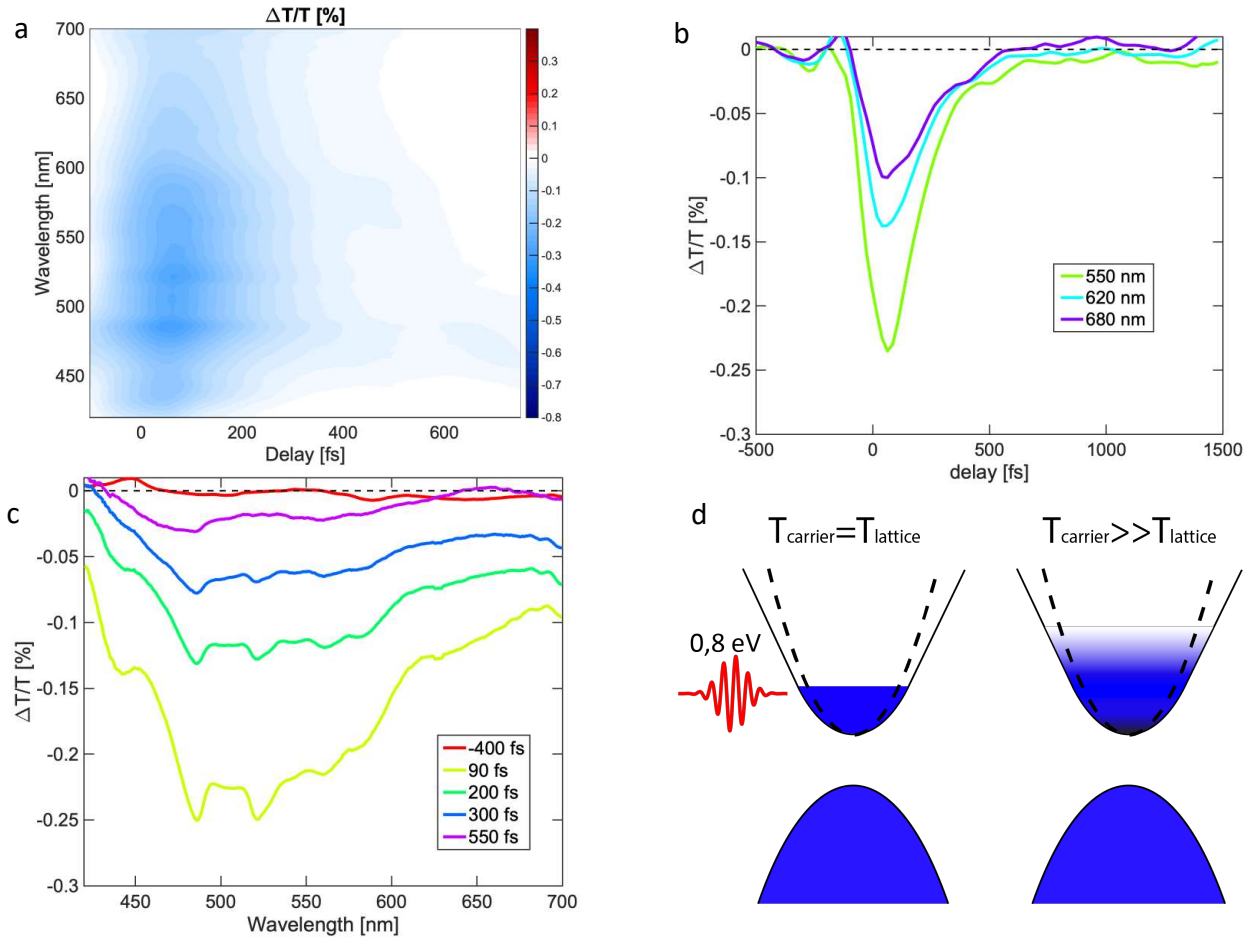

Figure 2 a) Differential transmission 2D map as a function of wavelength and time delay for the ITO film; b) Temporal behavior at 500 nm; c) Spectral evolution at different time delays; d) sketch of the intraband excitation in ITO and non-parabolicity of ITO band

Figure 2a shows color coded pump probe map in the range of 450-700nm, where we see a broad negative signal. In Figure 2b-2c we can see two different cuts of the map: in Figure 2b we plot the recovery dynamics at different wavelengths and we can see that we have a sub picosecond relaxation that is associated to electron-phonon scattering in ITO, while in Figure 2c we plot the evolution of the whole spectrum at some selected pump-probe delay. When exciting the electron gas of a metal with resonant light pulses an out of equilibrium distribution of hot electrons is created. In the first tens of femtoseconds the electrons thermalize to a hot Fermi-Dirac distribution with an electronic temperature $T_{carrier}>>T_{lattice}$. This gives the highest transient signal in ultrafast measurements. Thereafter, the hot electron distribution cools down to through electron-phonon scattering (Figure 2d), which results in the initial ultrafast decay observed in Figure 2c within the first picosecond of the measurement [18,19]. The second longer decay then is a result of the hot lattice after the carriers cooled down.

The fabrication of the ITO grating allows us a control of the ultrafast modulation of an optical signal in terms of either an increase (positive $\Delta T/T$) or a decrease (negative $\Delta T/T$) of light transmission through the sample. Such control is determined via the choice of the grating pitch. We show the

result of the intraband excitation measurement on the two gratings in Figure 3. In Figure 3a we can see that in this case we have a positive and a negative signal in the measurement, differently than in the case of ITO film. This change of transmission arises from the shift of transmission minima of the grating caused by an ultrafast modulation of the refractive index of the ITO. The dielectric permittivity, i.e. the square of the refractive index, of materials with a significant free carrier density, such as ITO, can be described well by the Drude function. This latter depends on the high frequency dielectric constant ε_∞ of the material and the plasma frequency ω_p, which itself is a function of the carrier density and the effective mass. Since intraband pumping does not excite any additional electron from the valence band, we are not changing the carrier density. The change of refractive index instead is associated to a change in the plasma frequency arising from a variation of the effective mass of the carriers *m**, due to the non-parabolicity of the conduction band of heavily doped semiconductors. In a parabolic band the associated effective mass is constant all along the band dispersion while in a non-parabolic one the effective mass depends on the energy of the carriers, and *m** increases with increasing energy [12]. In fact, this strong modulation of the photonic bandgap in the visible as observed by us is a result of an intense variation of the dielectric permittivity as a result of the effective mass variation of the hot carriers (and not the high frequency dielectric constant ε_∞ as in noble metals).[12] We further observed that we can modulate the spectral window of the ultrafast variation by controlling the fabrication parameters, giving us room for the direct design of signal modulation in the visible spectral range (see Figure S3 of the Supporting Information).

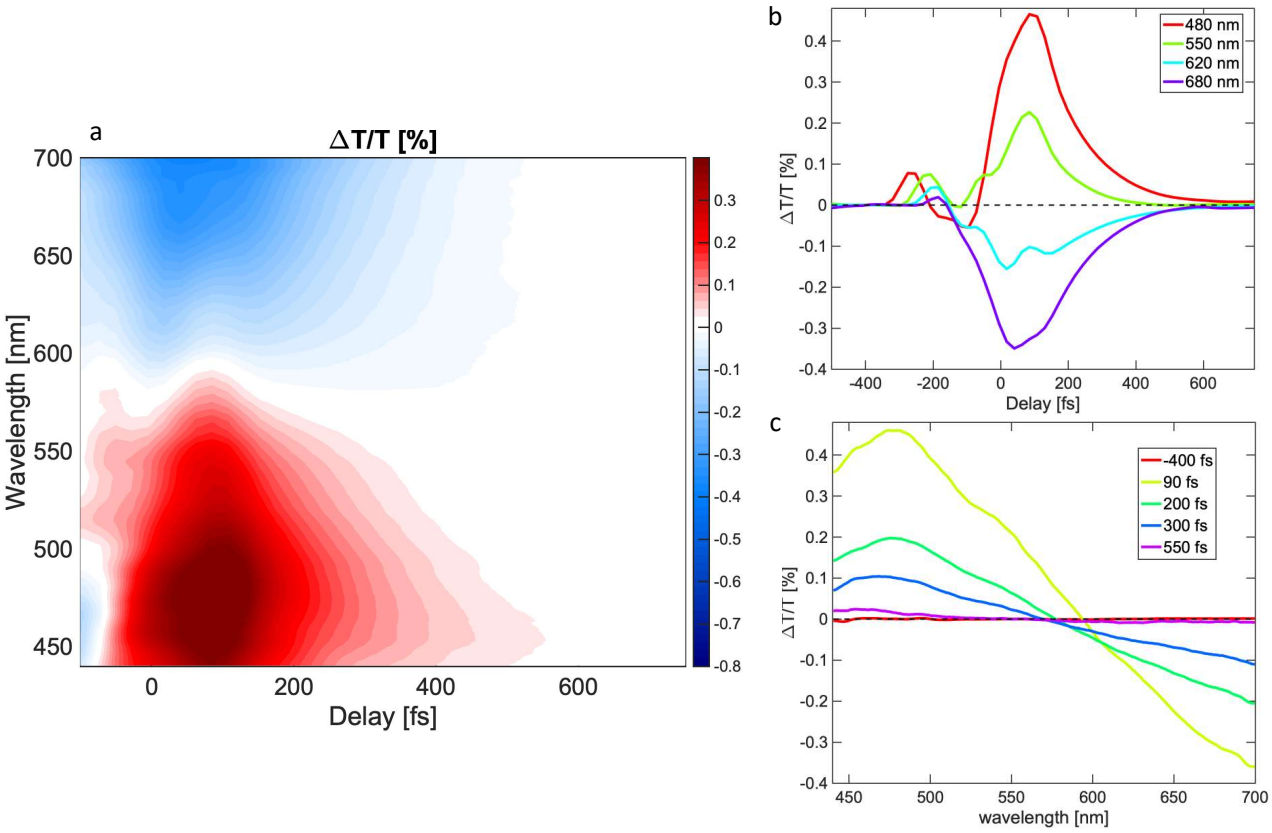

Figure 3 Intraband dynamics a) Differential transmission 2D map of the grating. b) Recovery dynamics of the grating c) Spectral evolution at different time delays;

The relaxation dynamics as seen in Figure 3b is driven by the electron cooling and is sub picosecond, resulting in a two orders of magnitude faster decay channel than in metals, e.g. gold.[20]The

presence of the glass behind the ITO causes the so called cross phase modulation (XPM) artifact. This can be seen in the dynamics where before the decay we have some unwanted modulation. Those are induced by the change of the refractive index in the glass caused by the huge amount of photons passing through.[21] This is not in any case changing the relaxation dynamics. The artifact does not have a proper dynamic and after the artifact is ended we have zero contribution from it.

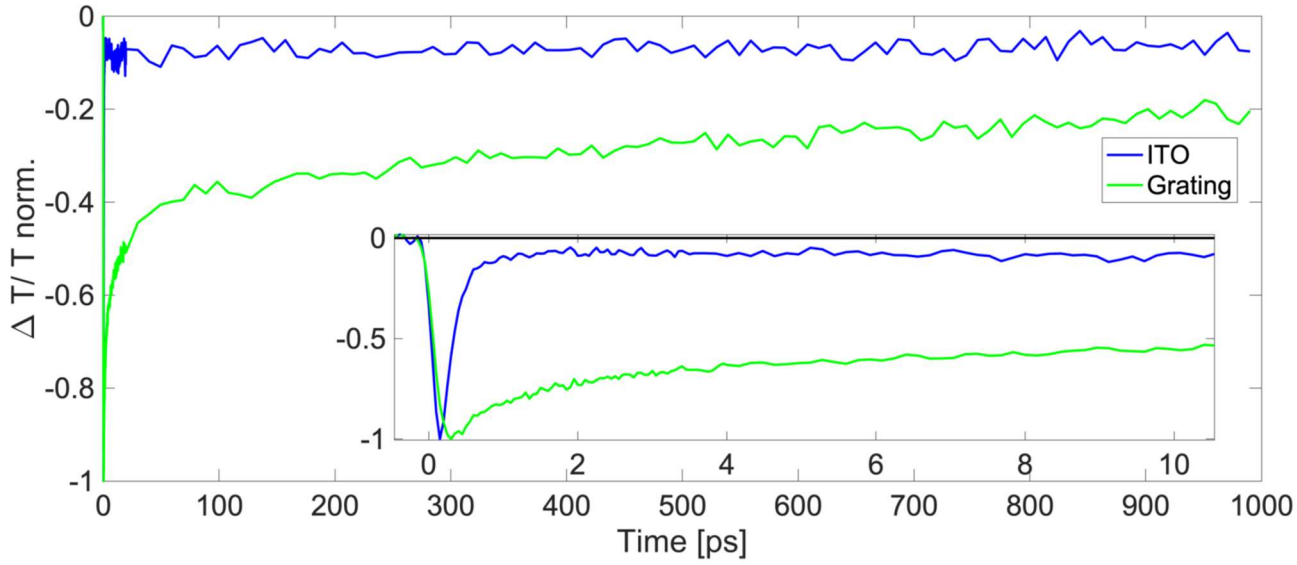

Figure 4 Interband dynamics, comparison of normalized decay at 550nm between thin film and ITO grating.

As a final investigation we pumped the interband transitions of ITO by using a pump pulse at 266 nm, which is beyond the bandgap of ITO. In this scenario the energy of the photons is enough to promote an electron from the valence to the conduction band. This results in an increase of the carrier density, which in turn lowers the plasma frequency ω_p and, thus, has an overall effect on the dielectric permittivity. The results for both, the thin films and the gratings are shown in Figure 4. For both cases a negative signal is observed corresponding to a decrease of the transmission. Notably, the ITO film in Figure 4 is governed by a sub picosecond decay, while the result from our grating appears to have a much slower decay. In the thin ITO film case the decay dynamic look very similar to what is observed in the intraband transition case, i.e. a two-step decay with an ultrafast component of less than 0.5 picoseconds, and a second slower one over several hundreds of picoseconds, which resembles strongly the direct excitation of the plasmon resonance. The usual process takes place: electron-electron scattering and electron phonon scattering, followed by the cooling of the lattice. This is a typical signal response of thin heavily doped metal oxide films.[22] It is notable that we are able to modify the signal response of the ITO film strongly by forming the grating structure. It appears that this structural arrangement strongly confined in width on the micrometer scale favors the excitation of the interband processes. This latter signal displays a signal build-up of about 150 femtoseconds, followed by an initial decay within the first 100 picoseconds. We interpret the results in the following way: The initial rise time is a result of the cooling of the hot carriers that were excited way beyond the bandgap to the edge of the conduction band of the material. The following exponential decay resembles strongly the electron-hole recombination of semiconductors (see Figure S4 of the Supporting Information).[23] Thereafter a long living signal is observed, which we assign to either the strong heating of the lattice due to the creation of the initial hot carriers, or, more likely, to the creation of trap states induced by the femtosecond laser micro-machining processes that changes the relaxation path of the electrons. Possibly, the trapping of the

carriers towards the surface of the fabricated structure extends the life time of the carriers and therefore favors the interband relaxation processes, observed by us in the grating structure and similar to what has been observed in other confined structures of heavily doped metal oxides.[23,24]

Conclusion

In conclusion, we demonstrate the fabrication of ITO grating structures with varying width and pitch distance via femtosecond laser micro machining. This technique allowed us creating large areas of periodic structures in the millimeter regime and therefore enables the work with laser beams with large beam waists, reducing the use of optical components. Our transient absorption measurements display an ultrafast signal modulation in the picosecond time scale. The formation of the grating structure delivers the opportunity to control exactly the signal wavelength and to induce transmission suppression as well enhancement in the visible spectral range as a result of the refractive index variation of ITO on the ultrafast timescale. Our results show that picosecond spectral modulation in the visible becomes accessible in ITO microarray structures on a scale of 5x5 mm fabricated by femtosecond laser micromachining, bringing this system closer to industrial relevance.

Acknowledgement

This project has received funding from the European Research Council (ERC) under the European Union's Horizon 2020 research and innovation programme (grant agreement No. [816313]).

References

[1] I. Kriegel, F. Scotognella, L. Manna, Plasmonic doped semiconductor nanocrystals: Properties, fabrication, applications and perspectives, Physics Reports. 674 (2017) 1–52. https://doi.org/10.1016/j.physrep.2017.01.003.

[2] A. Agrawal, R.W. Johns, D.J. Milliron, Control of Localized Surface Plasmon Resonances in Metal Oxide Nanocrystals, Annual Review of Materials Research. 47 (2017) 1–31. https://doi.org/10.1146/annurev-matsci-070616-124259.

[3] A. Comin, L. Manna, New materials for tunable plasmonic colloidal nanocrystals, Chem. Soc. Rev. 43 (2014) 3957–3975. https://doi.org/10.1039/C3CS60265F.

[4] F. Scotognella, G. Della Valle, A.R. Srimath Kandada, M. Zavelani-Rossi, S. Longhi, G. Lanzani, F. Tassone, Plasmonics in heavily-doped semiconductor nanocrystals, The European Physical Journal B. 86 (2013). https://doi.org/10.1140/epjb/e2013-40039-x.

[5] A.L. Routzahn, S.L. White, L.-K. Fong, P.K. Jain, Plasmonics with Doped Quantum Dots, Israel Journal of Chemistry. 52 (2012) 983–991. https://doi.org/10.1002/ijch.201200069.

[6] J.M. Luther, P.K. Jain, T. Ewers, A.P. Alivisatos, Localized surface plasmon resonances arising from free carriers in doped quantum dots, Nature Materials. 10 (2011) 361–366. https://doi.org/10.1038/nmat3004.

[7] P.P. Edwards, A. Porch, M.O. Jones, D.V. Morgan, R.M. Perks, Basic materials physics of transparent conducting oxides, Dalton Trans. (2004) 2995–3002. https://doi.org/10.1039/B408864F.

[8] N.R. Armstrong, P.A. Veneman, E. Ratcliff, D. Placencia, M. Brumbach, Oxide Contacts in Organic Photovoltaics: Characterization and Control of Near-Surface Composition in Indium−Tin Oxide (ITO) Electrodes, Acc. Chem. Res. 42 (2009) 1748–1757. https://doi.org/10.1021/ar900096f.

[9] M.Z. Alam, I.D. Leon, R.W. Boyd, Large optical nonlinearity of indium tin oxide in its epsilon-near-zero region, Science. 352 (2016) 795–797. https://doi.org/10.1126/science.aae0330.
[10] S.-Q. Li, P. Guo, D.B. Buchholz, W. Zhou, Y. Hua, T.W. Odom, J.B. Ketterson, L.E. Ocola, K. Sakoda, R.P.H. Chang, Plasmonic–Photonic Mode Coupling in Indium-Tin-Oxide Nanorod Arrays, ACS Photonics. 1 (2014) 163–172. https://doi.org/10.1021/ph400038g.
[11] D.B. Tice, S.-Q. Li, M. Tagliazucchi, D.B. Buchholz, E.A. Weiss, R.P.H. Chang, Ultrafast Modulation of the Plasma Frequency of Vertically Aligned Indium Tin Oxide Rods, Nano Lett. 14 (2014) 1120–1126. https://doi.org/10.1021/nl4028044.
[12] P. Guo, R.D. Schaller, J.B. Ketterson, R.P.H. Chang, Ultrafast switching of tunable infrared plasmons in indium tin oxide nanorod arrays with large absolute amplitude, Nature Photonics. 10 (2016) 267–273. https://doi.org/10.1038/nphoton.2016.14.
[13] P. Guo, R.D. Schaller, L.E. Ocola, B.T. Diroll, J.B. Ketterson, R.P.H. Chang, Large optical nonlinearity of ITO nanorods for sub-picosecond all-optical modulation of the full-visible spectrum, Nature Communications. 7 (2016) 12892. https://doi.org/10.1038/ncomms12892.
[14] P. Guo, R.P.H. Chang, R.D. Schaller, Transient Negative Optical Nonlinearity of Indium Oxide Nanorod Arrays in the Full-Visible Range, ACS Photonics. 4 (2017) 1494–1500. https://doi.org/10.1021/acsphotonics.7b00278.
[15] G.M. Paternò, C. Iseppon, A. D'Altri, C. Fasanotti, G. Merati, M. Randi, A. Desii, E.A.A. Pogna, D. Viola, G. Cerullo, F. Scotognella, I. Kriegel, Solution processable and optically switchable 1D photonic structures, ArXiv:1711.03192 [Cond-Mat, Physics:Physics]. (2017). http://arxiv.org/abs/1711.03192 (accessed December 6, 2017).
[16] S.L. Turco, A.D. Donato, L. Criante, Scattering effects of glass-embedded microstructures by roughness controlled fs-laser micromachining, J. Micromech. Microeng. 27 (2017) 065007. https://doi.org/10.1088/1361-6439/aa6b3b.
[17] G. Cerullo, C. Manzoni, L. Lüer, D. Polli, Time-resolved methods in biophysics. 4. Broadband pump–probe spectroscopy system with sub-20 fs temporal resolution for the study of energy transfer processes in photosynthesis, Photochem. Photobiol. Sci. 6 (2007) 135–144. https://doi.org/10.1039/B606949E.
[18] G.V. Hartland, Optical Studies of Dynamics in Noble Metal Nanostructures, Chemical Reviews. 111 (2011) 3858–3887. https://doi.org/10.1021/cr1002547.
[19] F. Scotognella, G. Della Valle, A.R. Srimath Kandada, D. Dorfs, M. Zavelani-Rossi, M. Conforti, K. Miszta, A. Comin, K. Korobchevskaya, G. Lanzani, L. Manna, F. Tassone, Plasmon Dynamics in Colloidal $Cu_{2-x}Se$ Nanocrystals, Nano Letters. 11 (2011) 4711–4717. https://doi.org/10.1021/nl202390s.
[20] S. Link, M.A. El-Sayed, Spectral Properties and Relaxation Dynamics of Surface Plasmon Electronic Oscillations in Gold and Silver Nanodots and Nanorods, J. Phys. Chem. B. 103 (1999) 8410–8426. https://doi.org/10.1021/jp9917648.
[21] M. Lorenc, M. Ziolek, R. Naskrecki, J. Karolczak, J. Kubicki, A. Maciejewski, Artifacts in femtosecond transient absorption spectroscopy, Appl Phys B. 74 (2002) 19–27. https://doi.org/10.1007/s003400100750.
[22] N. Kinsey, C. DeVault, J. Kim, M. Ferrera, V.M. Shalaev, A. Boltasseva, Epsilon-near-zero Al-doped ZnO for ultrafast switching at telecom wavelengths, Optica. 2 (2015) 616–622. https://doi.org/10.1364/OPTICA.2.000616.
[23] I. Kriegel, C. Urso, D. Viola, L. De Trizio, F. Scotognella, G. Cerullo, L. Manna, Ultrafast Photodoping and Plasmon Dynamics in Fluorine–Indium Codoped Cadmium Oxide Nanocrystals for All-Optical Signal Manipulation at Optical Communication Wavelengths, J. Phys. Chem. Lett. 7 (2016) 3873–3881. https://doi.org/10.1021/acs.jpclett.6b01904.

[24] B.T. Diroll, P. Guo, R.P.H. Chang, R.D. Schaller, Large Transient Optical Modulation of Epsilon-Near-Zero Colloidal Nanocrystals, ACS Nano. 10 (2016) 10099–10105. https://doi.org/10.1021/acsnano.6b05116.

Supporting Information

Large scale indium tin oxide (ITO) one dimensional gratings for ultrafast signal modulation in the visible

Michele Guizzardi, Silvio Bonfadini, Liliana Moscardi, Ilka Kriegel, Francesco Scotognella, Luigino Criante

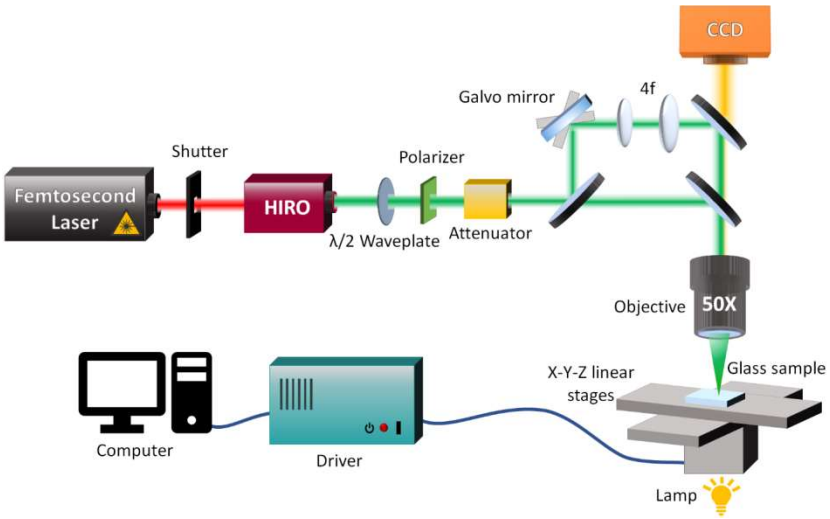

Figure S1. Sketch of the femtosecond laser micromachining apparatus

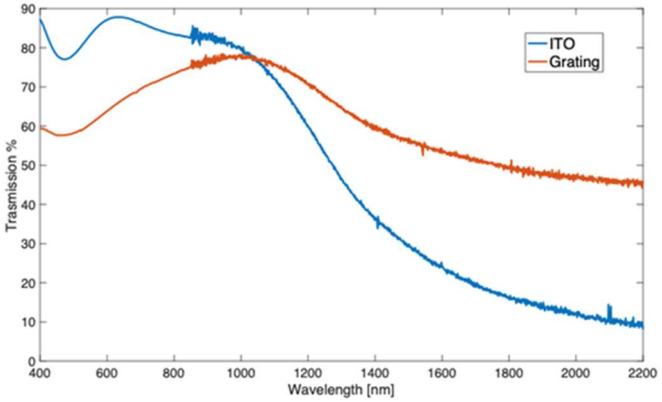

Figure S2. Transmission up to 2200 nm of ITO film and grating

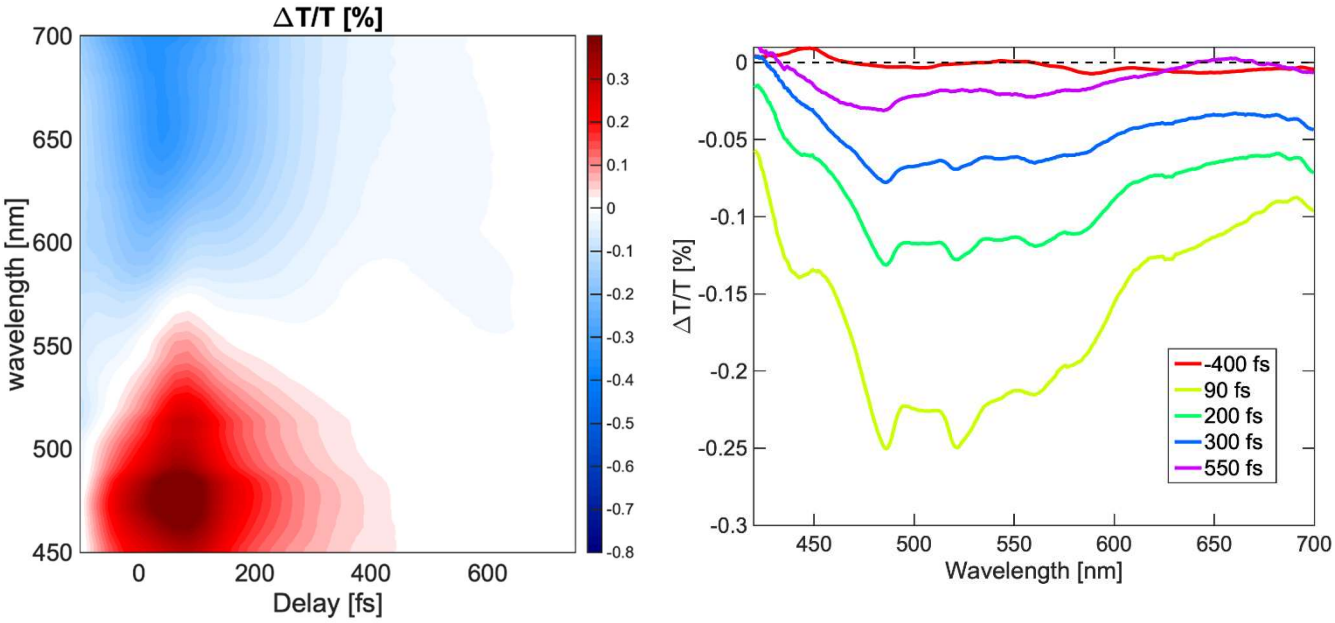

Figure S3. Differential transmission map and spectral evolution of the second grating.

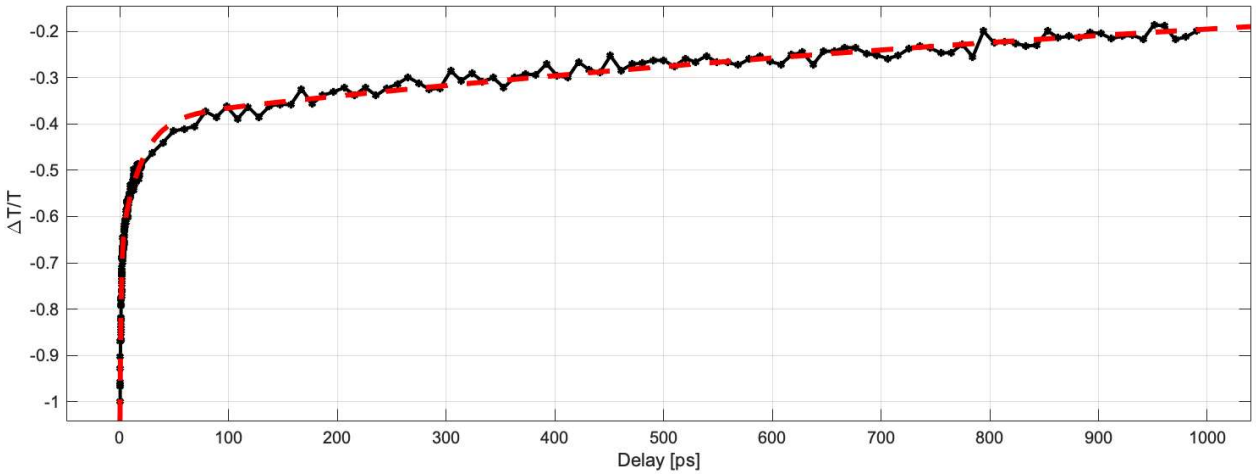

f(x) = -(a*exp(-x/d)+b*exp(-x/e)+c*exp(-x/f))
oefficients (with 95% confidence bounds):
a = 0.3987 (0.3811, 0.4163)
b = 0.2841 (0.2725, 0.2957)
c = 0.3904 (0.3835, 0.3973)
d = 1.112 (1.014, 1.21)
e = 18.52 (17.04, 20)
f = 1440 (1367, 1513)

Figure S4. Tri-exponential fit of the interband grating dynamic with the result of the fit.